



**HAL**  
open science

# Gasdermin and Gasdermin-Like Pore-Forming Proteins in Invertebrates, Fungi and Bacteria

Asen Daskalov, N. Louise Glass

► **To cite this version:**

Asen Daskalov, N. Louise Glass. Gasdermin and Gasdermin-Like Pore-Forming Proteins in Invertebrates, Fungi and Bacteria. *Journal of Molecular Biology*, 2022, 434 (4), pp.167273. 10.1016/j.jmb.2021.167273 . hal-04833196

**HAL Id: hal-04833196**

**<https://cnrs.hal.science/hal-04833196v1>**

Submitted on 12 Dec 2024

**HAL** is a multi-disciplinary open access archive for the deposit and dissemination of scientific research documents, whether they are published or not. The documents may come from teaching and research institutions in France or abroad, or from public or private research centers.

L'archive ouverte pluridisciplinaire **HAL**, est destinée au dépôt et à la diffusion de documents scientifiques de niveau recherche, publiés ou non, émanant des établissements d'enseignement et de recherche français ou étrangers, des laboratoires publics ou privés.

1 **Gasdermin and gasdermin-like pore-forming proteins in invertebrates,**  
2 **fungi and bacteria**

3  
4 Asen Daskalov<sup>1</sup> and N. Louise Glass<sup>2</sup>

5 <sup>1</sup>Institut de Biochimie et Génétique Cellulaires, University of Bordeaux, France and

6 <sup>2</sup>The Plant and Microbial Biology Department, The University of California, Berkeley,  
7 CA 94720-3102

8  
9 Corresponding Author

10 Asen Daskalov

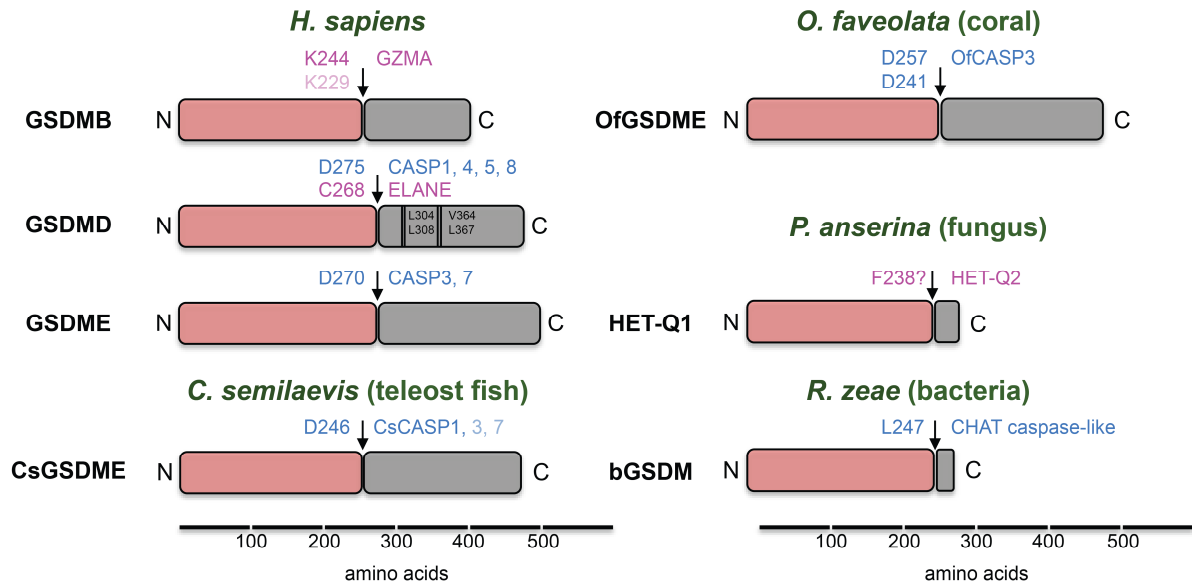
11 asen.daskalov@u-bordeaux.fr

12  
13  
14 **Keywords:**

15 Gasdermin, fungi, bacteria, pyroptosis, heterokaryon incompatibility, programmed cell death,  
16 innate immunity  
17  
18  
19

20 **Graphical Abstract**

21



22

23

24 **Research highlights**

25

- 26 • Gasdermin pore-formation as a key mechanism for cellular suicide
- 27 • Gasdermins in early diverged vertebrates and corals
- 28 • Fungal gasdermins and their regulation
- 29 • Gasdermins control cell death in Bacteria

30

31

32

33

34

35

36

37

38

39

40

41

42 **Abstract**

43

44         The gasdermin family of pore-forming proteins (PFPs) has recently emerged as  
45 key molecular players controlling immune-related cell death in mammals.  
46 Characterized mammalian gasdermins are activated through proteolytic cleavage by  
47 caspases or serine proteases, which remove an inhibitory carboxy-terminal domain,  
48 allowing the pore-formation process. Processed gasdermins form transmembrane  
49 pores permeabilizing the plasma membrane, which often results in lytic and  
50 inflammatory cell death. While the gasdermin-dependent cell death (*pyroptosis*) has  
51 been predominantly characterized in mammals, it now has become clear that  
52 gasdermins also control cell death in early vertebrates (teleost fish) and invertebrate  
53 animals such as corals (Cnidaria). Moreover, gasdermins and gasdermin-like proteins  
54 have been identified and characterized in taxa outside of animals, notably Fungi and  
55 Bacteria. Fungal and bacterial gasdermins share many features with mammalian  
56 gasdermins including their mode of activation through proteolysis. It has been shown  
57 that in some cases the proteolytic activation is executed by evolutionarily related  
58 proteases acting downstream of proteins resembling immune receptors controlling  
59 necroptosis in mammals. Overall, these findings establish gasdermins and gasdermin-  
60 regulated cell death as an extremely ancient mechanism of cellular suicide and build  
61 towards an understanding of the evolution of regulated cell death in the context of  
62 immunology. Here, we review the broader gasdermin family, focusing on recent  
63 discoveries in invertebrates, fungi and bacteria.

64

65

66

67

68

69

70

71

72

73

74

75

## 76 **Introduction**

77

78 Pore-formation is a general principle of membrane permeabilization integral  
79 to a variety of biological processes (i.e. immunity, virulence, metabolism) and  
80 performed by pore-forming proteins (PFPs) or toxins [1,2]. PFPs are ubiquitous  
81 throughout the tree of life and with diverse origins [1]. PFPs can be classified based  
82 on the secondary structure that the proteins use to permeabilize the lipid bilayer  
83 upon pore-formation [3,4]. The  $\alpha$ -PFPs use  $\alpha$ -helices for membrane insertion, while  
84  $\beta$ -PFPs use  $\beta$ -sheets [5,6]. Although structurally and phylogenetically diverse, PFPs  
85 share the ability to transit from a soluble state to a transmembrane and oligomeric  
86 state upon activation. Bacteria secrete soluble PFPs that kill other bacterial cells or  
87 that are used to invade and colonize a host [7,8]. These PFPs represents virulence  
88 factors, which attack the outer layer of the cellular membrane. Eukaryotes (i.e.  
89 cnidarians and arachnids) produce PFPs that are integral to their venomous toolkit  
90 and are used to attack prey or repel aggressors in a defense reaction [9,10].  
91 Actinoporins are an example of PFPs, and are found in the venom of a variety of sea  
92 anemones [11,12]. Mammals have also integrated pore-forming proteins into their  
93 immune systems [2,13]. Some mammalian PFPs can target directly the membranes of  
94 bacterial or viral pathogens, acting in the extracellular environment of the host [14],  
95 or targeting the outer membrane of phagocytosed Gram-negative bacteria [15]. The  
96 molecularly characterized PFPs in this category (i.e. *complement* members (C6-C9)  
97 [16] and perforin [17,18]), belong to the *membrane attack complex/perforin* (MACPF)  
98 superfamily [19]. The MACPF protein superfamily also includes the cholesterol-  
99 dependent cytolysins (CDCs) family [20] and pleurotolysine members [21] and is of  
100 ancient evolutionary origin with proteins found in eukaryotic, bacterial and archaeal  
101 lineages [19,22].

102 While MACPF members in mammals target cellular surfaces recognized as 'non  
103 self' (including damaged host cells), the mammalian immune system equally relies on  
104 PFPs integral to regulated cell death (RCD) programs – forms of cellular suicide –  
105 protecting the organism by eliminating infected and potentially harmful cells  
106 [2,23,24]. One such program of cellular suicide is the *intrinsic apoptotic pathway*,  
107 which relies on the pore-forming BAX and BAK proteins from the BCL-2 family

108 [25,26]. The BCL-2 family consist of ~20 members in mammals, which share a highly  
109 similar  $\alpha$ -helical fold [27,28]. Activated BAX/BAK proteins oligomerize into the  
110 mitochondrial outer membrane [29,30], which disrupts its integrity and leads to  
111 release of cytochrome c, triggering downstream activation of pro-apoptotic caspases  
112 (cysteine proteases) [31]. Similar to the MACPF superfamily, the BCL-2 family is of  
113 ancient evolutionary origin with members identified in early diverging metazoan  
114 phyla such as arthropods, mollusks and sponges [32,33].

115 In mammals, two other RCD pathways lead to permeabilization of the plasma  
116 membrane, resulting in inflammatory, immune-related forms of cell death, termed  
117 *necroptosis* and *pyroptosis* [2,34–36]. Necroptotic cell death is dependent on  
118 permeabilization of the plasma membrane by the MLKL protein (mixed lineage kinase  
119 domain-like) [37–39]. MLKL oligomerizes upon phosphorylation, which activates the  
120 N-terminal four-helical bundle (4HB) domain of the protein, carrying the cytotoxic  
121 activity, and inserts into the lipid bilayer of the plasma membrane [40,41]. The  
122 necroptotic pathway appears poorly conserved in Deuterostomia and is not present  
123 in Cnidaria [42]. However, MLKL homologs are present in most animal lineages and  
124 some viruses, which use decoy MLKL homologs to subvert the necroptotic cell death  
125 pathway and evade the mammalian immune system [43]. Furthermore, the pore-  
126 forming 4HB domain of MLKL appears homologous to immunity-related, membrane-  
127 targeting, cell death-inducing domains in fungi (HeLo and HELL domains) and in  
128 plants (RPW8-like coiled coil (CC) domain) [44–47]. The later findings underscore  
129 the broad phylogenetic distribution of this pore-forming protein domain.

130 In this review, we focus on the recently discovered cell death effectors of  
131 pyroptosis – the *gasdermin* family of PFPs – and detail the latest findings of  
132 gasdermin and gasdermin-like proteins characterized in organisms other than  
133 mammals (class Mammalia). Specifically, we will review molecularly characterized  
134 gasdermin proteins from invertebrates (Cnidaria), Fungi and Bacteria.

135

### 136 **Gasdermins – effectors of pyroptotic cell death in mammals**

137

138 Pyroptosis is a lytic, pro-inflammatory form of cell death in mammals [34,48].  
139 Gasdermins are a family of pore-forming proteins that play an essential role in  
140 pyroptosis by permeabilizing the plasma membrane during the cell death reaction

141 [49–51]. In humans, there are six gasdermin homologs (GSDMA, GSDMB, GSDMC,  
142 GSDMD, GSDME and PJVK – also known as DFNB59), while in mice the gasdermin  
143 family comprises 10 members with three GSDMA paralogs (GSDMA1-3), four GSDMC  
144 paralogs (GSDMC1-4) but no GSDMB homolog [49]. The gasdermin proteins are  
145 differentially expressed in various types of mammalian cells, although they share  
146 similar domain organization and a common mechanism of activation. Characterized  
147 mammalian gasdermins are two-domain proteins with a pore-forming N-terminal  
148 domain and a C-terminal repressor domain, which is removed by proteolytic cleavage  
149 to induce pyroptosis [49]. The C-terminal domain of GSDMD has been shown to play a  
150 crucial role in the recruitment of active caspases, which bind to it with high affinity  
151 [52,53]. Thus, the C-terminal domain of GSDMD is not only essential for inhibition of  
152 the cytotoxic activity of the protein but is also a caspase-recruitment module [52,53].  
153 The proteolysis of GSDMD by pro-inflammatory caspase-1 (or -4, -5 (human) and -11  
154 (mouse)) results in a 31-kDa N-terminal fragment (GSDMD-NT) and a 22-kDa C-  
155 terminal fragment (GSDMD-CT) [54–56]. GSDMD-NT interacts with negatively  
156 charged lipid heads on the inner side of the plasma membrane and oligomerizes to  
157 form transmembrane pores [57]. GSDMD pore-formation has been observed *in vitro*  
158 in the presence of liposomes and on hydrophilic mica surfaces [57–59] and recently  
159 the structure of the GSDMD pore has been obtained using cryo-EM (cryogenic  
160 electron microscopy) [60]. The GSDMD pore structure has a 33-mer toroidal pore,  
161 featuring a transmembrane  $\beta$ -barrel with inner diameter of ~22-nm (Fig. 1); each  
162 GSDMD monomer contributes with two  $\beta$ -hairpins (or four  $\beta$ -strand ‘fingers’ or  
163 ‘blades’ per monomer) [60]. GSDMD monomers also have a cytosolic globular domain,  
164 in addition to the domain (region) forming the transmembrane  $\beta$ -hairpins. The  
165 globular domains of the GSDMD molecules form a 40-nm high rim around the pore  
166 facing the inside of the cell, thus curving the plasma membrane around the pore  
167 towards the extracellular space [60]. GSDMD pore assemblies can have different  
168 symmetries – ranging from 31-fold to 34-fold symmetry – and are thus between 10-  
169 20% larger than previously characterized 27-fold symmetry GSDMA3 pores (Fig. 1)  
170 [61] and even larger than the estimated size of human GSDMB pores, averaging  
171 between 13.5-nm and 15.6-nm in pore diameter [62]. GSDMD pore-formation  
172 dynamics have been observed with time-lapse atomic force microscopy (AFM),

173 organizing in time-dependent manner from rearrangements of slit-, arc- and ring-  
174 shaped structures that are already inserted in the lipid bilayer [63].

175 Not all gasdermins are activated by inflammatory caspases. GSDME (DFNA5) is  
176 proteolytically processed by the pro-apoptotic caspase-3 (Fig. 2), to induce  
177 secondary necrotic cell death in cells undergoing apoptosis [64,65]. Caspase-3-  
178 mediated and GSDME-dependent pyroptotic cell death is proposed to play an  
179 important role in chemotherapeutic cancer treatments and is responsible for  
180 undesired secondary effects [65]. Recently, GSDMC has been identified as a substrate  
181 for the 'pro-apoptotic' caspase-8 [66]. CASP8 has been shown to cleave GSDMD in  
182 response to *Yersinia* (bacterial) effector protein YopJ, triggering pyroptosis in  
183 macrophages [67,68]. In neutrophils the response to *Yersinia* leads to pyroptosis  
184 through GSDME cleavage, which is CASP3-dependent [69]. While all three of these  
185 gasdermins (GSDMD, GSDME and GSDMC) are caspase substrates, another human  
186 gasdermin (GDSMB) has been identified as a substrate of a subtilisin-like serine  
187 protease named Granzyme A (GZMA) (Fig. 2) [70]. The protease is delivered into  
188 damaged or infected cells by natural killer (NK) lymphocytes, triggering GDSMB-  
189 dependent pyroptosis [70]. Interestingly, a different serine protease (ELANE) has  
190 been found to cleave GSDMD seven amino acid residues upstream of D275 (the  
191 identified caspase cleavage site) to induce lytic cell death in aging neutrophils [71].  
192 Remarkably, some mammalian gasdermins have also been reported as targets of viral  
193 proteases [72,73]. For example, human GSDMD can be proteolytically processed after  
194 amino acid Q193 by a C3 protease from the Enterovirus 71 (EV71), preventing  
195 pyroptosis and evading antiviral immunity [72]. Another cysteine protease of the  
196 same family, C3<sup>Pro</sup> from Seneca Valley virus (SVV), cleaves porcine GSDMD at residue  
197 Q277, generating a pyroptosis-inducing pGSDMD(1-277) fragment, which likely plays  
198 an important role in viral pathogenesis [73].

199

## 200 **Gasdermin proteins in early diverging vertebrates and corals**

201

202 The gasdermin family of PFPs has mostly been studied in vertebrates and  
203 specifically mammals. Phylogenetically, GSDME and PJVK are the two most ancient  
204 gasdermin genes in metazoans, found in early diverging vertebrate species (teleost  
205 fish) [74] and some invertebrates like corals [49,75]. Three of the gasdermins



206 (GSDMB, GSDMC, GSDMD) are exclusively found in mammals, while GSDMA is more  
207 ancient and is present in birds and reptiles [49]. The recent functional  
208 characterization of CsGSDME – a GSDME homolog from the tongue sole *Cynoglossus*  
209 *semilaevis* – has revealed that the gasdermin protein can induce pyroptotic cell death  
210 in human HEK293T cells, suggesting that CsGSDME is a pyroptosis executioner in this  
211 early group of vertebrates [74]. The N-terminal domain of CsGSDME is essential for  
212 the cell death reaction and exhibits bactericidal properties. Unlike the mammalian  
213 GSDME, whose activation depends on caspase-3 (CASP3), *C. semilaevis* GSDME is  
214 cleaved with highest affinity by CsCASP1 (caspase-1) and much less efficiently by  
215 caspase-3 and -7 (Fig. 2) [74]. GSDME homologs are also encoded in the genomes of  
216 some invertebrates, notably mollusks (*Lingula anatina* and *Pomacea canaliculata*),  
217 sea anemone (*Exaiptasia pallida*) and corals [75]. Jiang *et al.* recently characterized a  
218 gasdermin E homolog from the reef-building coral *Orbicella faveolata* [75]. The  
219 authors demonstrated that OfGSDME can be proteolytically processed *in vitro* by  
220 human caspase-3 and -7 and coral OfCASP3 can induce pyroptotic cell death in  
221 human HEK293T cells [75,76]. Similar to previously characterized gasdermin  
222 proteins, the cytotoxic activity of OfGSDME has been found to reside in its N-terminal  
223 pore-forming domain. In addition, Jiang *et al.* demonstrate that gasdermin E mediates  
224 pyroptosis *in vivo* in the coral species *Pocillopora damicornis* in response to bacterial  
225 infections. Polyps of *P. damicornis* undergo rapid necrotic cell death reaction when  
226 infected with *V. coralliilyticus* bacteria, during which PdGSDME is proteolytically  
227 processed in CASP3-dependent manner. These findings show that pyroptosis is an  
228 ancient mechanism controlling immune-related cell death in invertebrates and that  
229 some pyroptosis-inducing pathways are broadly conserved in divergent metazoan  
230 taxa [76].

231

### 232 **Gasdermin-like proteins in fungi**

233

234 Proteins belonging to the gasdermin family have also been identified in  
235 another major eukaryotic kingdom – Fungi – in the context of allorecognition-  
236 induced cell death [77,78]. Allorecognition (or conspecific non-self discrimination)  
237 occurs between genetically distinct fungal individuals (strains) and can manifest  
238 through localized regulated cellular death (RCD) of newly formed heterokaryotic

239 cells, resulting in abortive somatic fusions that prevent cytoplasmic mixing [77,79–  
240 81]. Allorecognition-mediated cell death has been shown to serve as a defense  
241 mechanism against genome exploitation [82], resource plundering [83] and the  
242 spread of cytoplasmic deleterious elements (i.e. mycoviruses and senescence  
243 plasmids) [84–86]. The fungal gasdermins have been identified and characterized as  
244 cell death executioner proteins in the context of allorecognition in two model  
245 ascomycete species, *Neurospora crassa* [78,87] and *Podospora anserina* [88]. Fungal  
246 gasdermin-encoding genes are widespread and abundant in the fungal kingdom,  
247 especially in the Ascomycota phylum [87,88].

248

249 *The gasdermin-like protein RCD-1 regulates cell death in the filamentous ascomycete*  
250 *Neurospora crassa*

251

252 The first identified fungal gasdermin, encoded in the genome of the model  
253 ascomycete *N. crassa*, has been named *rcd-1* (*regulator of cell death-1*) [78,87]. While  
254 the majority of identified *N. crassa* incompatibility genes appear to be inactive in the  
255 earliest developmental stages of somatic growth (spores or *conidia*) [89,90], the co-  
256 expression of two different *rcd-1* alleles (*rcd-1-1* and *rcd-1-2*) triggers rapid (~20  
257 min post-fusion) lytic cell death in germinating conidia (germlings) and in hyphae  
258 [87]. Germling-regulated death (GRD) occurs when conidia of the *rcd-1-1* genotype  
259 undergo somatic cell fusion with an *rcd-1-2* strain, resulting in progressively  
260 increasing vacuolization and subsequent release of cytoplasmic contents. The uptake  
261 of vital dyes (propidium iodide) by *N. crassa* germlings undergoing GRD suggested  
262 that plasma membrane integrity is compromised before cytoplasmic leakage [87].  
263 Alleles at the *rcd-1* locus are highly polymorphic, fall into two haplogroups and are  
264 associated with genomic re-arrangements in genome analyses of a wild population of  
265 *N. crassa*. The two antagonistic alleles (*rcd-1-1* and *rcd-1-2*) show molecular marks of  
266 evolution, notably long-term balancing selection and trans-species polymorphism,  
267 typically associated with allorecognition genes in fungi [91,92] and immune-related  
268 genes in animals [93–95] and plants [96].

269 The *rcd-1-1* and *rcd-1-2* alleles encode proteins of 257 and 244 amino acids,  
270 respectively, and exhibit a low level of sequence identity (38%) when aligned with  
271 each other [87]. The homology between the two RCD-1 variants and the mammalian

272 gasdermins was initially detected *in silico* using primary sequence alignments  
273 combined with secondary structure predictions [78]. The fungal gasdermins are  
274 evolutionary related to the pore-forming N-terminal domain of mammalian  
275 gasdermins and lack regions of similarity to the inhibitory C-terminal domain. Both  
276 allelic variants (RCD-1-1 and RCD-1-2) localize to the cell periphery and recombinant  
277 RCD-1 binds to negatively charged phospholipids *in vitro* [78]. The lipid-binding  
278 profile of fungal gasdermins and mammalian gasdermins are similar and consist of an  
279 affinity for cardiolipin (CL), phosphatidylserine (PS) and some phosphoinositides  
280 [59,78]. Liposomes containing CL and PS were lysed in presence of RCD-1. RCD-1 also  
281 shows a tendency to form oligomers of high molecular size *in vitro* and when  
282 observed by electron microscopy, RCD-1 oligomers formed irregularly sized cells  
283 resembling a honeycomb, suggesting that the fungal gasdermins might also form  
284 pore-like structures [78]. In accordance with these observations, GFP-labeled RCD-1  
285 proteins formed large ordered fluorescent aggregates in *N. crassa* germlings  
286 undergoing GRD, indicating that the fungal gasdermins oligomerize *in vivo*.  
287 Importantly, co-expression of RCD-1-1 and RCD-1-2 in human 293T induced  
288 pyroptotic-like cell death and the appearance of balloon-shaped dead cells [78].  
289 While the precise molecular details of the RCD-1-1/RCD-1-2 allorecognition system  
290 remain to be elucidated, it has been determined that the two allelic variants interact  
291 during the cell death reaction in the heterologous host (293T cells) [78]. These  
292 findings led to a proposed model in which the interaction between RCD-1-1 and RCD-  
293 1-2 leads to the formation of cytotoxic pore-like oligomers to permeabilize the  
294 plasma membrane and induce cell death. Overall, the molecular characterization of  
295 RCD-1 has established an evolutionary relationship between cell death execution  
296 modules in fungi and animals, showing that gasdermins operate as PFPs in  
297 Opisthokonta (the fungal and animal eukaryotic kingdoms).

298

### 299 *HET-Q1 and the proteolytic regulation of the fungal gasdermins*

300

301 In spite of the functional commonalities between mammalian and fungal  
302 gasdermins, it remained unclear what the precise mechanism controlling the  
303 cytotoxic activity of fungal gasdermins might be, especially considering that fungal  
304 gasdermins lack the inhibitory C-terminal domain found in mammalian gasdermins

305 and the apparent self-sufficiency of the RCD-1-1/RCD-1-2 cell death system in human  
306 293T cells. A recent study by Clavé *et al.* has shed light on this important question by  
307 showing that some fungal gasdermins, similar to their mammalian counterparts, are  
308 regulated through proteolytic cleavage [88]. By investigating the genetic  
309 determinants of an allorecognition system from *Podospora anserina* (a model  
310 ascomycete fungus), the authors identified a fungal gasdermin - HET-Q1 - a 278  
311 amino acid protein whose cytotoxicity is controlled by a subtilisin-like serine  
312 protease of the S8 family [97], named HET-Q2. The *het-Q1* and *het-Q2* genes are  
313 defined as idiomorphs [98]; different genes encoded in the same locus in the  
314 genomes of different strains, with strains being exclusively *het-Q1* or *het-Q2*  
315 genotypes. Similar to the GRD reaction in *N. crassa*, co-expression of HET-Q1 and  
316 HET-Q2 induced cell death of heterokaryotic cells. The cell death reaction occurred  
317 in mature hyphae and was observed via the appearance of a demarcation line (a  
318 'barrage') separating the incompatible *het-Q1* and *het-Q2* strains. The gasdermin  
319 HET-Q1 is proteolytically processed during the cell death reaction in a HET-Q2-  
320 dependent manner with removal of a ~5-kDa C-terminal fragment [88]. Although the  
321 precise cleavage site was not identified, mutational analysis of HET-Q1 showed that  
322 two residues - L237 and F238 - abolished cleavage of HET-Q1 and also abolished cell  
323 death, while the introduction of a HET-Q1(1-233) truncation variant was sufficient to  
324 reduce cell viability. These findings support that the cytotoxicity of HET-Q1 is  
325 activated through proteolytic cleavage of an inhibitory C-terminal domain. The HET-  
326 Q1/HET-Q2 allorecognition reaction had also been successfully recapitulated in the  
327 yeast *Saccharomyces cerevisiae* [88], suggesting that the HET-Q1 gasdermin is the  
328 direct substrate of the HET-Q2 serine protease.

329 Remarkably, genome-mining analyses revealed that ~80% of gasdermin-  
330 encoding genes in fungi are situated in the vicinity (10-kbp upstream or  
331 downstream) of a protease-encoding *het-Q2*-like gene and often formed *het-Q1/het-*  
332 *Q2*-like two-gene clusters [88]. The *het-Q2*-like genes encode multidomain proteins  
333 that exhibit a diversity of domain architectures, in which the predicted protease  
334 domain was frequently associated with structural repeats like TPR (tetratricopeptide  
335 repeat) [99], ANK (ankyrin) [100] and WD40 repeats [101]. Such short tandem-  
336 repeated sequences (between 30-45 amino acids) have been documented to form  
337 protein domains mediating protein-protein interactions in various kingdoms of life

338 [102]. Two main types of protease domains have been found associated with the  
339 HET-Q2-like proteins: subtilisin-like serine proteases of the S8 family and  
340 surprisingly, caspase-like CHAT protease domains [88,103]. Furthermore, some HET-  
341 Q2-like protein architectures belonged to the NOD-like family of immune receptors  
342 (or NLRs), which have been shown to control pyroptotic cell death in mammals [104]  
343 and cell death in other eukaryotes, including plants and fungi [105–107]. Fungal  
344 NLR-encoding genes have been previously reported to cluster genomically and to  
345 control the cytotoxic activity of downstream effectors, some of which are pore-  
346 forming toxins [107–109]. Based on these findings, it has been proposed that the  
347 HET-Q2-like proteins represent molecular sensors controlling the cytotoxic activity  
348 by proteolytic cleavage of fungal gasdermins [88]. Thus, the *het-Q1/het-Q2*-like gene  
349 clusters represent molecular pathways controlling immune-related cell death outside  
350 of allorecognition and likely in response to heterospecific non-self. Overall, the  
351 findings establish an unprecedented evolutionary relationship between immune-  
352 related cell death pathways in the animal and fungal kingdoms.

353 In light of the discovered proteolytic regulation of the fungal gasdermin-like  
354 proteins, the *rcd-1-1/rcd-1-2* allorecognition system from *N. crassa*, where the co-  
355 expression of two different gasdermin alleles triggers cell death [78], is puzzling.  
356 Some fungal allorecognition cell death-inducing systems have emerged from pre-  
357 existing signaling pathways through selected mutations [110,111], as allorecognition  
358 has fitness benefits [79,80]. RCD-1-1 and RCD-1-2 are shorter than the majority of  
359 fungal gasdermins, with RCD-1-2 being only 244 amino acids in length and lacking an  
360 inhibitory C-terminal domain [78,87]. Such alterations combined with additional  
361 factors (mutations) could have led to the emergence of the *rcd-1* incompatibility  
362 system. A similar scenario has been proposed for the *het-Q1/het-Q2* incompatibility  
363 system in *P. anserina*, which could have emerged from a *het-Q1/het-Q2*-like gene  
364 cluster with the HET-Q2-like protein losing its regulatory, inhibitory domain [88]  
365 (Fig. 3). Additional experimental data would be needed regarding the molecular  
366 details of fungal gasdermin/protease interactions, recognition and cleavage, to  
367 support the latter hypothesis. Although gasdermin homologs are widespread in  
368 fungal genomes, their evolutionary history, mechanism of activation and function in  
369 allorecognition or immunity has not been fully explored, with the exception of the  
370 two incompatibility systems (*rcd-1-1/rcd-1-2* and *het-Q1/het-Q2*). Further

371 experiments on these two model systems, as well on other gasdermin homologs in  
372 fungi, will be fruitful in defining the evolution and function of this enigmatic protein  
373 family.

374

### 375 **Gasdermin-like proteins in Bacteria**

376

377 In addition to fungi, gasdermin-encoding genes have been identified in  
378 prokaryotes, notably bacteria [78,87]. A recent study by Johnson *et al.* structurally  
379 and functionally characterized bacterial gasdermins, which were encoded in anti-  
380 phage defense islands in various bacterial genomes [112]. The authors identified  
381 approximately 50 gasdermin sequences from bacterial species, which formed a  
382 separate clade from the fungal and mammalian gasdermins. Yet, similar to the fungal  
383 gasdermins, the bacterial gasdermin sequences lack an extended inhibitory C-  
384 terminal domain. By obtaining crystal structures of two distantly related bacterial  
385 gasdermins (sharing only 18% sequence identity), Johnson *et al.* show that in spite of  
386 the extreme phylogenetic distance between the eukaryotic and prokaryotic taxa, the  
387 N-terminal cytotoxic domain of the bacterial and mammalian gasdermins exhibited  
388 remarkable structural homology in their inhibited state [112]. In both cases, a  
389 twisted central anti-parallel  $\beta$ -sheet represents the core of the fold, decorated on the  
390 periphery by connecting helices and strands, which showed also a good structural  
391 overlap between the gasdermin families. The high-resolution molecular structures  
392 also revealed the mechanism of auto-inhibition of the bacterial gasdermins, by  
393 exposing the role of the short C-terminal fragment, which is positioned in the middle  
394 of the twisted central  $\beta$ -sheet, likely stabilizing the inhibited state of the protein. In  
395 addition, the structural analyses revealed that some bacterial gasdermins undergo  
396 post-translational modification at their extreme N-terminal end, involving a  
397 conserved cysteine residue (C3 or C4 in the sequences of the two crystalized  
398 bacterial gasdermins). The authors determined that the cysteine sidechain is  
399 palmitoylated and that this modification plays an important role in the stability of  
400 the protein fold [112]. These findings thus elucidate the minimal requirements for  
401 the inhibited inactive state of the bacterial gasdermins. Palmitoylation may also be  
402 important in some fungal gasdermins, as they carry a conserved N-terminal cysteine  
403 [112].

404 Genome mining analyses by Johnson *et al.* revealed that the bacterial  
405 gasdermin genes, as described for the fungal gasdermin genes, are genomically  
406 clustered with protease-encoding genes. Furthermore, several different types of  
407 putative protease domains were identified, including caspase-like domains of the  
408 CHAT (Pfam ID PF12770) and C14 (PF00656) families and subtilisin-like serine  
409 proteases. Some of the predicted protein architectures carrying protease domains,  
410 represent bacterial NLRs or NLR-like proteins [112]. Importantly, Johnson *et al.*  
411 demonstrate that co-expression of the bacterial gasdermins and their cognate  
412 proteases leads to bacterial growth arrest and membrane permeabilization. The  
413 cytotoxic activity of the bacterial gasdermins relies on the proteolytic cleavage of the  
414 C-terminal inhibitory fragment (Fig. 2), thus triggering the formation of highly  
415 ordered ring-like pores. *In vitro*, in presence of liposomes, the ring-like pores  
416 assembled into mesh-like supramolecular structures. Surprisingly, the pores formed  
417 by the bacterial gasdermins exhibited significantly larger inner diameter (200-300 Å)  
418 than the inner diameter of pores formed by the mammalian gasdermins (125-200 Å)  
419 [112]. In the future, atomic-level structural characterization of the bacterial pores  
420 would be needed to compare in detail the molecular mechanism of pore-formation  
421 between the bacterial, fungal and metazoan gasdermins.

422

## 423 **Conclusion**

424

425 The discovery of gasdermin-like pore-forming proteins outside of mammals  
426 and vertebrates indicates that the gasdermin family is of extremely old evolutionary  
427 origin and likely a core-component of innate immune systems in divergent eukaryotic  
428 and prokaryotic taxa. These findings are emerging in the context of the establishment  
429 of an elaborate anti-viral (phage) bacterial immune system [113] with several recent  
430 studies reporting evolutionary parallels between bacterial and mammalian anti-viral  
431 defense systems [114,115]. For example, proteins from the viperin family [114,116]  
432 or cyclic GMP-AMP synthase (cGAS) [115] produce antiviral nucleotide-derived  
433 metabolites in both bacteria and mammals. Furthermore, prokaryotic anti-viral  
434 immune systems rely on a large variety of enzymatic activities and yet to be  
435 characterized defense modules [117,118]. The discovery of gasdermins in bacteria –  
436 although their anti-phage defense activity is only hypothesized – suggests that some

437 PFPs are integral to a core of immune-related domains operating in eukaryotes and  
438 prokaryotes. In this context, it has recently been proposed that NLR-dependent  
439 amyloid-controlled cell death [109], which has been previously characterized in  
440 fungi and found to be evolutionary related to mammalian necroptosis [44], operates  
441 also in prokaryotes, notably multicellular bacteria [119]. However, additional  
442 experimental analyses are needed to determine if the membrane-targeting abilities of  
443 the bacterial cell death-inducing BELL domain [119] is analogous to the 4HB domain  
444 of the necroptosis executioner protein MLKL [40]. Taken together, these findings  
445 indicate that cellular suicide by pore-formation and membrane disruption is a  
446 widespread strategy of organismal defense, which can rely on evolutionary related  
447 cell death modules, like the gasdermin family, in eukaryotic and prokaryotic lineages.  
448 The conserved mode of regulation (proteolysis), which is executed by evolutionary  
449 related proteases under the control of homologous receptors, suggest that  
450 pyroptotic-like cell death pathways have played an important role throughout a  
451 significant part of natural history. Future research will explore the precise molecular  
452 cues and mechanisms that trigger gasdermin-dependent cell death in these diverse  
453 and distantly-related taxa (fungi and bacteria). Such endeavors will provide valuable  
454 details on the biological processes in which gasdermin-dependent pathways are  
455 involved, and will be a great contribution to the field of comparative immunology.

456

## 457 **References**

458

- 459 [1] Dal Peraro M, van der Goot FG. Pore-forming toxins: ancient, but never really  
460 out of fashion. *Nat Rev Microbiol* 2016;14:77–92. doi:10.1038/nrmicro.2015.3.
- 461 [2] Flores-Romero H, Ros U, Garcia-Saez AJ. Pore formation in regulated cell  
462 death. *EMBO J* 2020;39:e105753. doi:10.15252/embj.2020105753.
- 463 [3] Ros U, García-Sáez AJ. More Than a Pore: The Interplay of Pore-Forming  
464 Proteins and Lipid Membranes. *J Membr Biol* 2015;248:545–61.  
465 doi:10.1007/s00232-015-9820-y.
- 466 [4] Parker MW, Feil SC. Pore-forming protein toxins: from structure to function.  
467 *Prog Biophys Mol Biol* 2005;88:91–142.  
468 doi:10.1016/j.pbiomolbio.2004.01.009.
- 469 [5] Iacovache I, Bischofberger M, van der Goot FG. Structure and assembly of  
470 pore-forming proteins. *Curr Opin Struct Biol* 2010;20:241–6.  
471 doi:10.1016/j.sbi.2010.01.013.
- 472 [6] Boyd CM, Bubeck D. Advances in cryoEM and its impact on  $\beta$ -pore forming  
473 proteins. *Curr Opin Struct Biol* 2018;52:41–9. doi:10.1016/j.sbi.2018.07.010.
- 474 [7] Bischofberger M, Iacovache I, van der Goot FG. Pathogenic pore-forming  
475 proteins: function and host response. *Cell Host Microbe* 2012;12:266–75.



- 476 doi:10.1016/j.chom.2012.08.005.
- 477 [8] Gonzalez MR, Bischofberger M, Pernot L, van der Goot FG, Frêche B. Bacterial  
478 pore-forming toxins: the (w)hole story? *Cell Mol Life Sci* 2008;65:493–507.  
479 doi:10.1007/s00018-007-7434-y.
- 480 [9] Rivera-de-Torre E, Palacios-Ortega J, Gavilanes JG, Martínez-Del-Pozo Á,  
481 García-Linares S. Pore-Forming Proteins from Cnidarians and Arachnids as  
482 Potential Biotechnological Tools. *Toxins (Basel)* 2019;11.  
483 doi:10.3390/toxins11060370.
- 484 [10] Podobnik M, Anderluh G. Pore-forming toxins in Cnidaria. *Semin Cell Dev Biol*  
485 2017;72:133–41. doi:10.1016/j.semcdb.2017.07.026.
- 486 [11] Macrander J, Daly M. Evolution of the Cytolytic Pore-Forming Proteins  
487 (Actinoporins) in Sea Anemones. *Toxins (Basel)* 2016;8.  
488 doi:10.3390/toxins8120368.
- 489 [12] Palacios-Ortega J, Rivera-de-Torre E, García-Linares S, Gavilanes JG, Martínez-  
490 Del-Pozo Á, Slotte JP. Oligomerization of Sticholysins from Förster Resonance  
491 Energy Transfer. *Biochemistry* 2021;60:314–23.  
492 doi:10.1021/acs.biochem.0c00840.
- 493 [13] Tang D, Kang R, Berghe TV, Vandenabeele P, Kroemer G. The molecular  
494 machinery of regulated cell death. *Cell Res* 2019;29:347–64.  
495 doi:10.1038/s41422-019-0164-5.
- 496 [14] Dunkelberger JR, Song W-C. Complement and its role in innate and adaptive  
497 immune responses. *Cell Res* 2010;20:34–50. doi:10.1038/cr.2009.139.
- 498 [15] Merselis LC, Rivas ZP, Munson GP. Breaching the Bacterial Envelope: The  
499 Pivotal Role of Perforin-2 (MPEG1) Within Phagocytes. *Front Immunol*  
500 2021;12:597951. doi:10.3389/fimmu.2021.597951.
- 501 [16] Dudkina NV, Spicer BA, Reboul CF, Conroy PJ, Lukoyanova N, Elmlund H, et al.  
502 Structure of the poly-C9 component of the complement membrane attack  
503 complex. *Nat Commun* 2016;7:10588. doi:10.1038/ncomms10588.
- 504 [17] Law RHP, Lukoyanova N, Voskoboinik I, Caradoc-Davies TT, Baran K, Dunstone  
505 MA, et al. The structural basis for membrane binding and pore formation by  
506 lymphocyte perforin. *Nature* 2010;468:447–51. doi:10.1038/nature09518.
- 507 [18] Ni T, Jiao F, Yu X, Aden S, Ginger L, Williams SI, et al. Structure and mechanism  
508 of bactericidal mammalian perforin-2, an ancient agent of innate immunity. *Sci*  
509 *Adv* 2020;6:eaax8286. doi:10.1126/sciadv.aax8286.
- 510 [19] Moreno-Hagelsieb G, Vitug B, Medrano-Soto A, Saier MH. The membrane attack  
511 complex/perforin superfamily. *J Mol Microbiol Biotechnol* 2017;27:252–67.  
512 doi:10.1159/000481286.
- 513 [20] Gilbert RJC. Cholesterol-dependent cytolysins. *Adv Exp Med Biol* 2010;677:56–  
514 66. doi:10.1007/978-1-4419-6327-7\_5.
- 515 [21] Lukoyanova N, Kondos SC, Farabella I, Law RHP, Reboul CF, Caradoc-Davies  
516 TT, et al. Conformational changes during pore formation by the perforin-  
517 related protein pleurotolysin. *PLoS Biol* 2015;13:e1002049.  
518 doi:10.1371/journal.pbio.1002049.
- 519 [22] Anderluh G, Kisovec M, Kraševc N, Gilbert RJC. Distribution of MACPF/CDC  
520 proteins. *Subcell Biochem* 2014;80:7–30. doi:10.1007/978-94-017-8881-6\_2.
- 521 [23] Legrand AJ, Konstantinou M, Goode EF, Meier P. The diversification of cell  
522 death and immunity: memento mori. *Mol Cell* 2019;76:232–42.  
523 doi:10.1016/j.molcel.2019.09.006.
- 524 [24] Galluzzi L, Vitale I, Aaronson SA, Abrams JM, Adam D, Agostinis P, et al.  
525 Molecular mechanisms of cell death: recommendations of the Nomenclature

526 Committee on Cell Death 2018. *Cell Death Differ* 2018;25:486–541.  
527 doi:10.1038/s41418-017-0012-4.

528 [25] Peña-Blanco A, García-Sáez AJ. Bax, Bak and beyond - mitochondrial  
529 performance in apoptosis. *FEBS J* 2018;285:416–31. doi:10.1111/febs.14186.

530 [26] Czabotar PE, Lessene G, Strasser A, Adams JM. Control of apoptosis by the  
531 BCL-2 protein family: implications for physiology and therapy. *Nat Rev Mol*  
532 *Cell Biol* 2014;15:49–63. doi:10.1038/nrm3722.

533 [27] Kale J, Osterlund EJ, Andrews DW. BCL-2 family proteins: changing partners in  
534 the dance towards death. *Cell Death Differ* 2018;25:65–80.  
535 doi:10.1038/cdd.2017.186.

536 [28] Kvensakul M, Hinds MG. The Bcl-2 family: structures, interactions and targets  
537 for drug discovery. *Apoptosis* 2015;20:136–50. doi:10.1007/s10495-014-1051-  
538 7.

539 [29] Ugarte-Urbe B, García-Sáez AJ. Apoptotic foci at mitochondria: in and around  
540 Bax pores. *Philos Trans R Soc Lond B, Biol Sci* 2017;372.  
541 doi:10.1098/rstb.2016.0217.

542 [30] Salvador-Gallego R, Mund M, Cosentino K, Schneider J, Unsay J, Schraermeyer  
543 U, et al. Bax assembly into rings and arcs in apoptotic mitochondria is linked to  
544 membrane pores. *EMBO J* 2016;35:389–401. doi:10.15252/embj.201593384.

545 [31] Li J, Yuan J. Caspases in apoptosis and beyond. *Oncogene* 2008;27:6194–206.  
546 doi:10.1038/onc.2008.297.

547 [32] Strasser A, Vaux DL. Viewing BCL2 and cell death control from an evolutionary  
548 perspective. *Cell Death Differ* 2018;25:13–20. doi:10.1038/cdd.2017.145.

549 [33] Banjara S, Suraweera CD, Hinds MG, Kvensakul M. The Bcl-2 Family: Ancient  
550 Origins, Conserved Structures, and Divergent Mechanisms. *Biomolecules*  
551 2020;10. doi:10.3390/biom10010128.

552 [34] Shi J, Gao W, Shao F. Pyroptosis: Gasdermin-Mediated Programmed Necrotic  
553 Cell Death. *Trends Biochem Sci* 2017;42:245–54.  
554 doi:10.1016/j.tibs.2016.10.004.

555 [35] de Almagro MC, Vucic D. Necroptosis: Pathway diversity and characteristics.  
556 *Semin Cell Dev Biol* 2015;39:56–62. doi:10.1016/j.semcdb.2015.02.002.

557 [36] Kolbrink B, Riebeling T, Kunzendorf U, Krautwald S. Plasma membrane pores  
558 drive inflammatory cell death. *Front Cell Dev Biol* 2020;8:817.  
559 doi:10.3389/fcell.2020.00817.

560 [37] Wang H, Sun L, Su L, Rizo J, Liu L, Wang L-F, et al. Mixed lineage kinase  
561 domain-like protein MLKL causes necrotic membrane disruption upon  
562 phosphorylation by RIP3. *Mol Cell* 2014;54:133–46.  
563 doi:10.1016/j.molcel.2014.03.003.

564 [38] Samson AL, Zhang Y, Geoghegan ND, Gavin XJ, Davies KA, Mlodzianoski MJ, et  
565 al. MLKL trafficking and accumulation at the plasma membrane control the  
566 kinetics and threshold for necroptosis. *Nat Commun* 2020;11:3151.  
567 doi:10.1038/s41467-020-16887-1.

568 [39] Dondelinger Y, Declercq W, Montessuit S, Roelandt R, Goncalves A, Bruggeman  
569 I, et al. MLKL compromises plasma membrane integrity by binding to  
570 phosphatidylinositol phosphates. *Cell Rep* 2014;7:971–81.  
571 doi:10.1016/j.celrep.2014.04.026.

572 [40] Hildebrand JM, Tanzer MC, Lucet IS, Young SN, Spall SK, Sharma P, et al.  
573 Activation of the pseudokinase MLKL unleashes the four-helix bundle domain  
574 to induce membrane localization and necroptotic cell death. *Proc Natl Acad Sci*  
575 *USA* 2014;111:15072–7. doi:10.1073/pnas.1408987111.

- 576 [41] Petrie EJ, Sandow JJ, Jacobsen AV, Smith BJ, Griffin MDW, Lucet IS, et al.  
577 Conformational switching of the pseudokinase domain promotes human MLKL  
578 tetramerization and cell death by necroptosis. *Nat Commun* 2018;9:2422.  
579 doi:10.1038/s41467-018-04714-7.
- 580 [42] Dondelinger Y, Hulpiau P, Saeys Y, Bertrand MJM, Vandenabeele P. An  
581 evolutionary perspective on the necroptotic pathway. *Trends Cell Biol*  
582 2016;26:721–32. doi:10.1016/j.tcb.2016.06.004.
- 583 [43] Petrie EJ, Sandow JJ, Lehmann WIL, Liang L-Y, Coursier D, Young SN, et al.  
584 Viral MLKL homologs subvert necroptotic cell death by sequestering cellular  
585 RIPK3. *Cell Rep* 2019;28:3309–3319.e5. doi:10.1016/j.celrep.2019.08.055.
- 586 [44] Daskalov A, Habenstein B, Sabaté R, Berbon M, Martinez D, Chaignepain S, et  
587 al. Identification of a novel cell death-inducing domain reveals that fungal  
588 amyloid-controlled programmed cell death is related to necroptosis. *Proc Natl*  
589 *Acad Sci USA* 2016;113:2720–5. doi:10.1073/pnas.1522361113.
- 590 [45] Wang J, Hu M, Wang J, Qi J, Han Z, Wang G, et al. Reconstitution and structure  
591 of a plant NLR resistosome conferring immunity. *Science* 2019;364.  
592 doi:10.1126/science.aav5870.
- 593 [46] Barragan CA, Wu R, Kim S-T, Xi W, Habring A, Haggmann J, et al. RPW8/HR  
594 repeats control NLR activation in *Arabidopsis thaliana*. *PLoS Genet*  
595 2019;15:e1008313. doi:10.1371/journal.pgen.1008313.
- 596 [47] Seuring C, Greenwald J, Wasmer C, Wepf R, Saupe SJ, Meier BH, et al. The  
597 mechanism of toxicity in HET-S/HET-s prion incompatibility. *PLoS Biol*  
598 2012;10:e1001451. doi:10.1371/journal.pbio.1001451.
- 599 [48] Bergsbaken T, Fink SL, Cookson BT. Pyroptosis: host cell death and  
600 inflammation. *Nat Rev Microbiol* 2009;7:99–109. doi:10.1038/nrmicro2070.
- 601 [49] Broz P, Pelegrín P, Shao F. The gasdermins, a protein family executing cell  
602 death and inflammation. *Nat Rev Immunol* 2020;20:143–57.  
603 doi:10.1038/s41577-019-0228-2.
- 604 [50] Kovacs SB, Miao EA. Gasdermins: effectors of pyroptosis. *Trends Cell Biol*  
605 2017;27:673–84. doi:10.1016/j.tcb.2017.05.005.
- 606 [51] Ramos-Junior ES, Morandini AC. Gasdermin: A new player to the  
607 inflammasome game. *Biomed J* 2017;40:313–6. doi:10.1016/j.bj.2017.10.002.
- 608 [52] Liu Z, Wang C, Yang J, Chen Y, Zhou B, Abbott DW, et al. Caspase-1 Engages  
609 Full-Length Gasdermin D through Two Distinct Interfaces That Mediate  
610 Caspase Recruitment and Substrate Cleavage. *Immunity* 2020;53:106–114.e5.  
611 doi:10.1016/j.immuni.2020.06.007.
- 612 [53] Wang K, Sun Q, Zhong X, Zeng M, Zeng H, Shi X, et al. Structural mechanism for  
613 GSDMD targeting by autoprocessed caspases in pyroptosis. *Cell* 2020;180:941–  
614 955.e20. doi:10.1016/j.cell.2020.02.002.
- 615 [54] Shi J, Zhao Y, Wang K, Shi X, Wang Y, Huang H, et al. Cleavage of GSDMD by  
616 inflammatory caspases determines pyroptotic cell death. *Nature*  
617 2015;526:660–5. doi:10.1038/nature15514.
- 618 [55] Kayagaki N, Stowe IB, Lee BL, O'Rourke K, Anderson K, Warming S, et al.  
619 Caspase-11 cleaves gasdermin D for non-canonical inflammasome signalling.  
620 *Nature* 2015;526:666–71. doi:10.1038/nature15541.
- 621 [56] He W, Wan H, Hu L, Chen P, Wang X, Huang Z, et al. Gasdermin D is an executor  
622 of pyroptosis and required for interleukin-1 $\beta$  secretion. *Cell Res*  
623 2015;25:1285–98. doi:10.1038/cr.2015.139.
- 624 [57] Sborgi L, Rühl S, Mulvihill E, Pipercevic J, Heilig R, Stahlberg H, et al. GSDMD  
625 membrane pore formation constitutes the mechanism of pyroptotic cell death.

- 626 EMBO J 2016;35:1766–78. doi:10.15252/embj.201694696.
- 627 [58] Aglietti RA, Estevez A, Gupta A, Ramirez MG, Liu PS, Kayagaki N, et al. GsdmD  
628 p30 elicited by caspase-11 during pyroptosis forms pores in membranes. Proc  
629 Natl Acad Sci USA 2016;113:7858–63. doi:10.1073/pnas.1607769113.
- 630 [59] Ding J, Wang K, Liu W, She Y, Sun Q, Shi J, et al. Pore-forming activity and  
631 structural autoinhibition of the gasdermin family. Nature 2016;535:111–6.  
632 doi:10.1038/nature18590.
- 633 [60] Xia S, Zhang Z, Magupalli VG, Pablo JL, Dong Y, Vora SM, et al. Gasdermin D  
634 pore structure reveals preferential release of mature interleukin-1. Nature  
635 2021;593:607–11. doi:10.1038/s41586-021-03478-3.
- 636 [61] Ruan J, Xia S, Liu X, Lieberman J, Wu H. Cryo-EM structure of the gasdermin A3  
637 membrane pore. Nature 2018;557:62–7. doi:10.1038/s41586-018-0058-6.
- 638 [62] Hansen JM, de Jong MF, Wu Q, Zhang L-S, Heisler DB, Alto LT, et al. Pathogenic  
639 ubiquitination of GSDMB inhibits NK cell bactericidal functions. Cell  
640 2021;184:3178–3191.e18. doi:10.1016/j.cell.2021.04.036.
- 641 [63] Mulvihill E, Sborgi L, Mari SA, Pfreundschuh M, Hiller S, Müller DJ. Mechanism  
642 of membrane pore formation by human gasdermin-D. EMBO J 2018;37.  
643 doi:10.15252/embj.201798321.
- 644 [64] Rogers C, Fernandes-Alnemri T, Mayes L, Alnemri D, Cingolani G, Alnemri ES.  
645 Cleavage of DFNA5 by caspase-3 during apoptosis mediates progression to  
646 secondary necrotic/pyroptotic cell death. Nat Commun 2017;8:14128.  
647 doi:10.1038/ncomms14128.
- 648 [65] Wang Y, Gao W, Shi X, Ding J, Liu W, He H, et al. Chemotherapy drugs induce  
649 pyroptosis through caspase-3 cleavage of a gasdermin. Nature 2017;547:99–  
650 103. doi:10.1038/nature22393.
- 651 [66] Zhang J-Y, Zhou B, Sun R-Y, Ai Y-L, Cheng K, Li F-N, et al. The metabolite  $\alpha$ -KG  
652 induces GSDMC-dependent pyroptosis through death receptor 6-activated  
653 caspase-8. Cell Res 2021. doi:10.1038/s41422-021-00506-9.
- 654 [67] Sarhan J, Liu BC, Muendlein HI, Li P, Nilson R, Tang AY, et al. Caspase-8  
655 induces cleavage of gasdermin D to elicit pyroptosis during Yersinia infection.  
656 Proc Natl Acad Sci USA 2018;115:E10888–97. doi:10.1073/pnas.1809548115.
- 657 [68] Orning P, Weng D, Starheim K, Ratner D, Best Z, Lee B, et al. Pathogen  
658 blockade of TAK1 triggers caspase-8-dependent cleavage of gasdermin D and  
659 cell death. Science 2018;362:1064–9. doi:10.1126/science.aau2818.
- 660 [69] Chen KW, Demarco B, Ramos S, Heilig R, Goris M, Grayczyk JP, et al. RIPK1  
661 activates distinct gasdermins in macrophages and neutrophils upon pathogen  
662 blockade of innate immune signaling. Proc Natl Acad Sci USA 2021;118.  
663 doi:10.1073/pnas.2101189118.
- 664 [70] Zhou Z, He H, Wang K, Shi X, Wang Y, Su Y, et al. Granzyme A from cytotoxic  
665 lymphocytes cleaves GSDMB to trigger pyroptosis in target cells. Science  
666 2020;368. doi:10.1126/science.aaz7548.
- 667 [71] Kambara H, Liu F, Zhang X, Liu P, Bajrami B, Teng Y, et al. Gasdermin D Exerts  
668 Anti-inflammatory Effects by Promoting Neutrophil Death. Cell Rep  
669 2018;22:2924–36. doi:10.1016/j.celrep.2018.02.067.
- 670 [72] Lei X, Zhang Z, Xiao X, Qi J, He B, Wang J. Enterovirus 71 Inhibits Pyroptosis  
671 through Cleavage of Gasdermin D. J Virol 2017;91. doi:10.1128/JVI.01069-17.
- 672 [73] Wen W, Li X, Wang H, Zhao Q, Yin M, Liu W, et al. Seneca valley virus 3C  
673 protease induces pyroptosis by directly cleaving porcine gasdermin D. J  
674 Immunol 2021. doi:10.4049/jimmunol.2001030.
- 675 [74] Jiang S, Gu H, Zhao Y, Sun L. Teleost gasdermin E is cleaved by caspase 1, 3,

- 676 and 7 and induces pyroptosis. *J Immunol* 2019;203:1369–82.  
677 doi:10.4049/jimmunol.1900383.
- 678 [75] Jiang S, Zhou Z, Sun Y, Zhang T, Sun L. Coral gasdermin triggers pyroptosis. *Sci*  
679 *Immunol* 2020;5. doi:10.1126/sciimmunol.abd2591.
- 680 [76] Zhang Z, Lieberman J. Lighting a fire on the reef. *Sci Immunol* 2020;5.  
681 doi:10.1126/sciimmunol.abf0905.
- 682 [77] Gonçalves AP, Heller J, Rico-Ramírez AM, Daskalov A, Rosenfield G, Glass NL.  
683 Conflict, competition, and cooperation regulate social interactions in  
684 filamentous fungi. *Annu Rev Microbiol* 2020. doi:10.1146/annurev-micro-  
685 012420-080905.
- 686 [78] Daskalov A, Mitchell PS, Sandstrom A, Vance RE, Glass NL. Molecular  
687 characterization of a fungal gasdermin-like protein. *Proc Natl Acad Sci USA*  
688 2020.
- 689 [79] Daskalov A, Heller J, Herzog S, Fleißner A, Glass NL. Molecular mechanisms  
690 regulating cell fusion and heterokaryon formation in filamentous fungi. In:  
691 Heitman J, Howlett BJ, Crous PW, Stukenbrock EH, James TY, Gow NAR, editors.  
692 *The Fungal Kingdom*, Washington, DC, USA: ASM Press; 2017, p. 215–29.  
693 doi:10.1128/9781555819583.ch10.
- 694 [80] Paoletti M. Vegetative incompatibility in fungi: From recognition to cell death,  
695 whatever does the trick. *Fungal Biol Rev* 2016;30:152–62.  
696 doi:10.1016/j.fbr.2016.08.002.
- 697 [81] Glass NL, Kaneko I. Fatal attraction: nonself recognition and heterokaryon  
698 incompatibility in filamentous fungi. *Eukaryotic Cell* 2003;2:1–8.  
699 doi:10.1128/EC.2.1.1-8.2003.
- 700 [82] Bastiaans E, Debets AJM, Aanen DK. Experimental evolution reveals that high  
701 relatedness protects multicellular cooperation from cheaters. *Nat Commun*  
702 2016;7:11435. doi:10.1038/ncomms11435.
- 703 [83] Debets AJM, Griffiths AJF. Polymorphism of het-genes prevents resource  
704 plundering in *Neurospora crassa*. *Mycol Res* 1998;102:1343–9.  
705 doi:10.1017/S095375629800639X.
- 706 [84] Zhang D-X, Spiering MJ, Dawe AL, Nuss DL. Vegetative incompatibility loci with  
707 dedicated roles in allorecognition restrict mycovirus transmission in chestnut  
708 blight fungus. *Genetics* 2014;197:701–14. doi:10.1534/genetics.114.164574.
- 709 [85] Zhang D-X, Nuss DL. Engineering super mycovirus donor strains of chestnut  
710 blight fungus by systematic disruption of multilocus vic genes. *Proc Natl Acad*  
711 *Sci USA* 2016;113:2062–7. doi:10.1073/pnas.1522219113.
- 712 [86] Debets F, Yang X, Griffiths AJF. Vegetative incompatibility in *Neurospora*: its  
713 effect on horizontal transfer of mitochondrial plasmids and senescence in  
714 natural populations. *Curr Genet* 1994;26:113–9. doi:10.1007/BF00313797.
- 715 [87] Daskalov A, Gladieux P, Heller J, Glass NL. Programmed Cell Death in  
716 *Neurospora crassa* Is Controlled by the Allorecognition Determinant rcd-1.  
717 *Genetics* 2019;213:1387–400. doi:10.1534/genetics.119.302617.
- 718 [88] Clave C, Dyrka W, Granger-Farbos A, Pinson B, Saupe SJ, Daskalov A. Fungal  
719 gasdermin-like proteins are controlled by proteolytic cleavage. *BioRxiv* 2021.  
720 doi:10.1101/2021.06.03.446900.
- 721 [89] Shiu PK, Glass NL. Molecular characterization of tol, a mediator of mating-  
722 type-associated vegetative incompatibility in *Neurospora crassa*. *Genetics*  
723 1999;151:545–55.
- 724 [90] Ishikawa FH, Souza EA, Shoji J-Y, Connolly L, Freitag M, Read ND, et al.  
725 Heterokaryon incompatibility is suppressed following conidial anastomosis

- 726 tube fusion in a fungal plant pathogen. *PLoS One* 2012;7:e31175.  
 727 doi:10.1371/journal.pone.0031175.
- 728 [91] Zhao J, Gladieux P, Hutchison E, Bueche J, Hall C, Perraudeau F, et al.  
 729 Identification of Allorecognition Loci in *Neurospora crassa* by Genomics and  
 730 Evolutionary Approaches. *Mol Biol Evol* 2015;32:2417–32.  
 731 doi:10.1093/molbev/msv125.
- 732 [92] Milgroom MG, Smith ML, Drott MT, Nuss DL. Balancing selection at nonself  
 733 recognition loci in the chestnut blight fungus, *Cryphonectria parasitica*,  
 734 demonstrated by trans-species polymorphisms, positive selection, and even  
 735 allele frequencies. *Heredity* 2018;121:511–23. doi:10.1038/s41437-018-0060-  
 736 7.
- 737 [93] Nydam ML, Stephenson EE, Waldman CE, De Tomaso AW. Balancing selection  
 738 on allorecognition genes in the colonial ascidian *Botryllus schlosseri*. *Dev*  
 739 *Comp Immunol* 2017;69:60–74. doi:10.1016/j.dci.2016.12.006.
- 740 [94] Těšický M, Vinkler M. Trans-Species Polymorphism in Immune Genes: General  
 741 Pattern or MHC-Restricted Phenomenon? *J Immunol Res* 2015;2015:838035.  
 742 doi:10.1155/2015/838035.
- 743 [95] Kloch A, Wenzel MA, Laetsch DR, Michalski O, Bajer A, Behnke JM, et al.  
 744 Signatures of balancing selection in toll-like receptor (TLRs) genes - novel  
 745 insights from a free-living rodent. *Sci Rep* 2018;8:8361. doi:10.1038/s41598-  
 746 018-26672-2.
- 747 [96] Koenig D, Hagmann J, Li R, Bemm F, Slotte T, Neuffer B, et al. Long-term  
 748 balancing selection drives evolution of immunity genes in *Capsella*. *Elife*  
 749 2019;8. doi:10.7554/eLife.43606.
- 750 [97] Rawlings ND, Barrett AJ, Bateman A. MEROPS: the peptidase database. *Nucleic*  
 751 *Acids Res* 2010;38:D227–33. doi:10.1093/nar/gkp971.
- 752 [98] Glass NL, Grotelueschen J, Metzberg RL. *Neurospora crassa* A mating-type  
 753 region. *Proc Natl Acad Sci USA* 1990;87:4912–6.
- 754 [99] Zeytuni N, Zarivach R. Structural and functional discussion of the tetra-trico-  
 755 peptide repeat, a protein interaction module. *Structure* 2012;20:397–405.  
 756 doi:10.1016/j.str.2012.01.006.
- 757 [100] Li J, Mahajan A, Tsai M-D. Ankyrin repeat: a unique motif mediating protein-  
 758 protein interactions. *Biochemistry* 2006;45:15168–78.  
 759 doi:10.1021/bi062188q.
- 760 [101] Stirnimann CU, Petsalaki E, Russell RB, Müller CW. WD40 proteins propel  
 761 cellular networks. *Trends Biochem Sci* 2010;35:565–74.  
 762 doi:10.1016/j.tibs.2010.04.003.
- 763 [102] Jernigan KK, Bordenstein SR. Tandem-repeat protein domains across the tree  
 764 of life. *PeerJ* 2015;3:e732. doi:10.7717/peerj.732.
- 765 [103] Aravind L, Koonin EV. Classification of the caspase-hemoglobinase fold:  
 766 detection of new families and implications for the origin of the eukaryotic  
 767 separins. *Proteins* 2002;46:355–67. doi:10.1002/prot.10060.
- 768 [104] Andrade WA, Zamboni DS. NLRC4 biology in immunity and inflammation. *J*  
 769 *Leukoc Biol* 2020;108:1117–27. doi:10.1002/JLB.3MR0420-573R.
- 770 [105] Jones JDG, Vance RE, Dangl JL. Intracellular innate immune surveillance  
 771 devices in plants and animals. *Science* 2016;354. doi:10.1126/science.aaf6395.
- 772 [106] Mermigka G, Sarris PF. The rise of plant resistosomes. *Trends Immunol*  
 773 2019;40:670–3. doi:10.1016/j.it.2019.05.008.
- 774 [107] Dyrka W, Lamacchia M, Durrens P, Kobe B, Daskalov A, Paoletti M, et al.  
 775 Diversity and variability of NOD-like receptors in fungi. *Genome Biol Evol*

776 2014;6:3137–58. doi:10.1093/gbe/evu251.

777 [108] Daskalov A, Paoletti M, Ness F, Saupe SJ. Genomic clustering and homology  
778 between HET-S and the NWD2 STAND protein in various fungal genomes. *PLoS*  
779 *One* 2012;7:e34854. doi:10.1371/journal.pone.0034854.

780 [109] Daskalov A, Habenstein B, Martinez D, Debets AJM, Sabaté R, Loquet A, et al.  
781 Signal transduction by a fungal NOD-like receptor based on propagation of a  
782 prion amyloid fold. *PLoS Biol* 2015;13:e1002059.  
783 doi:10.1371/journal.pbio.1002059.

784 [110] Daskalov A, Saupe SJ. As a toxin dies a prion comes to life: A tentative natural  
785 history of the [Het-s] prion. *Prion* 2015;9:184–9.  
786 doi:10.1080/19336896.2015.1038018.

787 [111] Daskalov A, Dyrka W, Saupe SJ. 6 NLR Function in Fungi as Revealed by the  
788 Study of Self/Non-self Recognition Systems. In: Benz JP, Schipper K, editors.  
789 *Genetics and Biotechnology*, Cham: Springer International Publishing; 2020, p.  
790 123–41. doi:10.1007/978-3-030-49924-2\_6.

791 [112] Johnson AG, Wein T, Mayer ML, Duncan-Lowey B, Yirmiya E, Oppenheimer-  
792 Shaanan Y, et al. Bacterial gasdermins reveal an ancient mechanism of cell  
793 death. *BioRxiv* 2021. doi:10.1101/2021.06.07.447441.

794 [113] Bernheim A, Sorek R. The pan-immune system of bacteria: antiviral defence as  
795 a community resource. *Nat Rev Microbiol* 2020;18:113–9. doi:10.1038/s41579-  
796 019-0278-2.

797 [114] Bernheim A, Millman A, Ofir G, Meitav G, Avraham C, Shomar H, et al.  
798 Prokaryotic viperins produce diverse antiviral molecules. *Nature*  
799 2021;589:120–4. doi:10.1038/s41586-020-2762-2.

800 [115] Cohen D, Melamed S, Millman A, Shulman G, Oppenheimer-Shaanan Y, Kacen A,  
801 et al. Cyclic GMP-AMP signalling protects bacteria against viral infection.  
802 *Nature* 2019;574:691–5. doi:10.1038/s41586-019-1605-5.

803 [116] Minton K. Viperin breaks viral chains. *Nat Rev Immunol* 2018;18:480–1.  
804 doi:10.1038/s41577-018-0035-1.

805 [117] Gao L, Altae-Tran H, Böhning F, Makarova KS, Segel M, Schmid-Burgk JL, et al.  
806 Diverse enzymatic activities mediate antiviral immunity in prokaryotes.  
807 *Science* 2020;369:1077–84. doi:10.1126/science.aba0372.

808 [118] Whiteley AT, Eaglesham JB, de Oliveira Mann CC, Morehouse BR, Lowey B,  
809 Nieminen EA, et al. Bacterial cGAS-like enzymes synthesize diverse nucleotide  
810 signals. *Nature* 2019;567:194–9. doi:10.1038/s41586-019-0953-5.

811 [119] Dyrka W, Coustou V, Daskalov A, Lends A, Bardin T, Berbon M, et al.  
812 Identification of NLR-associated Amyloid Signaling Motifs in Bacterial  
813 Genomes. *J Mol Biol* 2020;432:6005–27. doi:10.1016/j.jmb.2020.10.004.

814

815

816

817

818

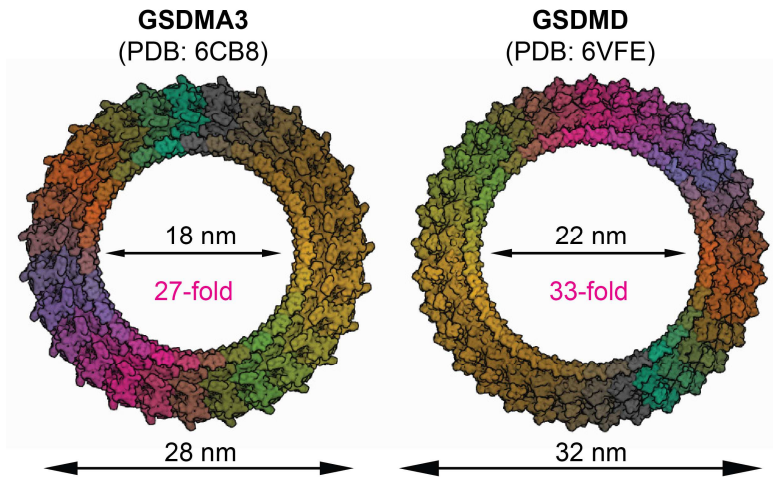
819

820

821

822

823 **Figures**

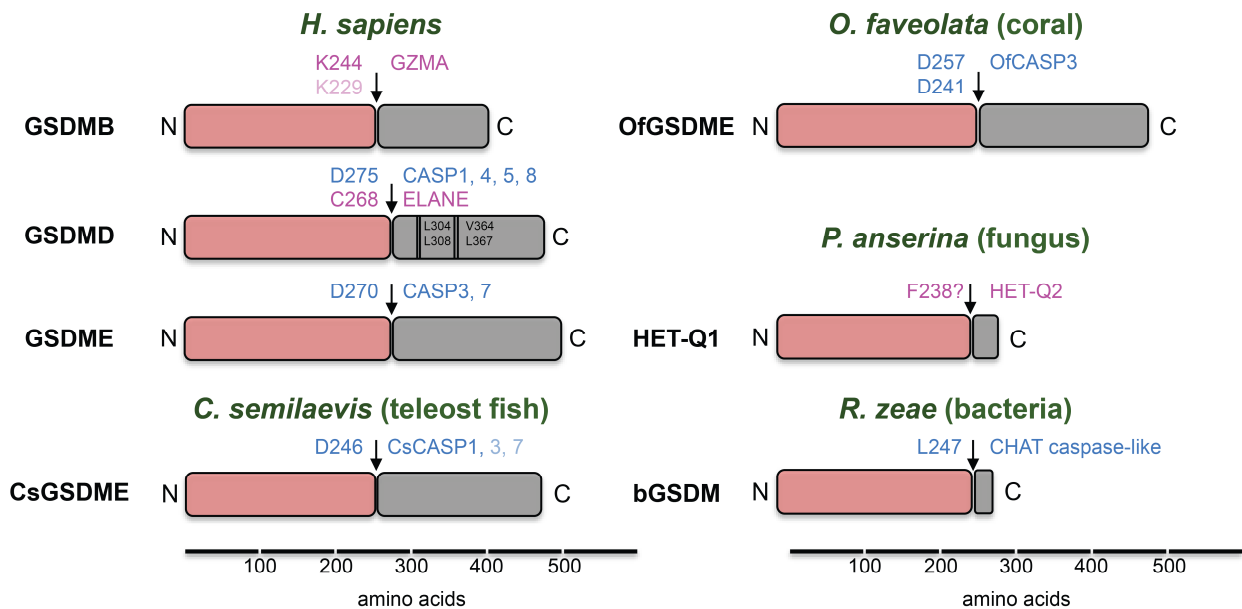


824

825 **Figure 1.** Structures of gasdermin pores formed by murine GSDMA3 (PDB: 6CB8) and  
826 human GSDMD (PDB: 6VFE) and obtained by cryo-EM [61]. Different gasdermin  
827 monomers are shown in different colors.

828

829

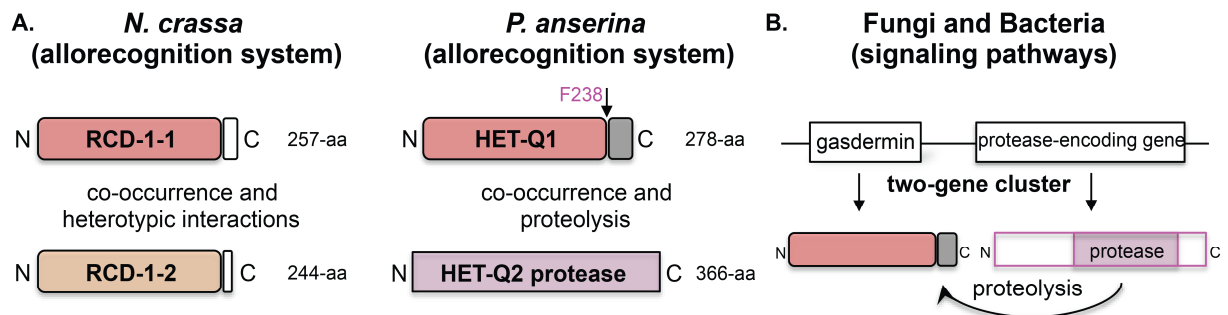


830

831 **Figure 2.** Shown are cartoons of gasdermin proteins from diverse phylogenetic taxa.  
832 The N-terminal pore-forming domains are colored in salmon pink. Cleavage sites are  
833 indicated with black arrows, flanked by the amino acid residues after which each



834 gasdermin is proteolytically processed and the proteases responsible for the  
 835 cleavage. Caspases and caspase-like proteases are shown in dark blue, while serine  
 836 proteases are shown in fuchsia. Color intensity indicates preferential cleavage sites  
 837 and/or higher cleavage affinity by a protease. Shown are four key amino acid  
 838 residues (L304, L308, V364, L367) on GSDMD C-terminal domain, which play a key  
 839 role in recruitment of caspase-1 and other inflammatory caspases. *H. sapiens* – *Homo*  
 840 *sapiens*, *C. semilaevis* – *Cynoglossus semilaevis*, *O. faveolata* – *Orbicella faveolata*, *P.*  
 841 *anserina* – *Podospora anserina*, *R. zeae* – *Runella zeae*.  
 842  
 843



844  
 845

846 **Figure 3. Gasdermin proteins are widespread in fungi and bacteria.** **A.**  
 847 Gasdermin-based alleloreognition systems in fungi. Presently, two different fungal  
 848 alleloreognition systems have been identified in two model fungal organisms –  
 849 *Neurospora crassa* and *Podospora anserina*. Cartoons represent the cell death-  
 850 inducing incompatibility factors (RCD-1-1/RCD-1-2 and HET-Q1/HET-Q2), which are  
 851 expressed by different fungal strains. The incompatibility factors occur in the same  
 852 cell only when different fungal colonies undergo somatic fusion (co-occurrence). The  
 853 RCD-1 alleloreognition system involves the heterotypic interaction between the two  
 854 antagonistic allelic variants RCD-1-1 and RCD-1-2. The two variants lack inhibitory  
 855 C-terminal domains as indicated by white boxes. The gray box shows the inhibitory  
 856 C-terminal domain of the HET-Q1 gasdermin. **B.** Gasdermin dependent signaling  
 857 pathways have been uncovered in filamentous fungi and bacteria. The gasdermin-  
 858 encoding genes are usually clustered with protease-encoding genes and represent  
 859 functional units.  
 860  
 861